# Unconventional elasticity in smectic-*A* elastomers

Olaf Stenull*
*Fachbereich Physik, Universität Duisburg-Essen, Campus Duisburg, 47048 Duisburg, Germany*

T. C. Lubensky
*Department of Physics and Astronomy, University of Pennsylvania, Philadelphia, Pennsylvania 19104, USA*

(Received 31 January 2006; revised manuscript received 30 April 2007; published 18 July 2007)

We study two aspects of the elasticity of smectic-*A* elastomers that make these materials genuinely and qualitatively different from conventional uniaxial rubbers. Under strain applied parallel to the layer normal, monodomain smectic-*A* elastomers exhibit a drastic change in Young's modulus above a threshold strain value of about 3%, as has been measured in experiments by [Nishikawa and Finkelmann, Macromol. Chem. Phys. **200**, 312 (1999)]. Our theory predicts that such strains induce a transition to a smectic-*C*-like state and that it is this transition that causes the change in elastic modulus. We calculate the stress-strain behavior as well as the tilt of the smectic layers and the molecular orientation for strain along the layer normal, and we compare our findings with the experimental data. We also study the electroclinic effect in chiral smectic-$A^*$ elastomers. According to experiments by [Lehmann *et al.*, Nature (London) **410**, 447 (2001)] and [Köhler *et al.*, Appl. Phys. A **80**, 381 (2003)], this effect leads in smectic-$A^*$ elastomers to a giant or, respectively, at least very large lateral electrostriction. Incorporating polarization into our theory, we calculate the height change of smectic-$A^*$ elastomer films in response to a lateral external electric field, and we compare this result to the experimental findings.

DOI: 10.1103/PhysRevE.76.011706 PACS number(s): 61.30.−v, 83.80.Va, 42.70.Df

## I. INTRODUCTION

Smectic elastomers [1] are rubbery materials that have the macroscopic symmetry properties of smectic liquid crystals [2]. They possess a planelike, lamellar modulation of density in one direction. In the smectic-*A* (Sm*A*) phase, the Frank director **n** describing the average orientation of constituent mesogens is parallel to the normal **N** of the smectic layers whereas in the smectic-*C* (Sm*C*) phase, it has a component in the plane of the layers. Monodomain Sm*A* elastomers are macroscopically uniaxial elastomers, albeit with unusual mechanical and electrical properties. For example, when strained along an axis normal to smectic layers, they exhibit a reorientation of smectic layers and an associated decrease in Young's modulus $Y_\parallel$ along this axis above a critical strain. This phenomenon, discovered experimentally by Nishikawa and Finkelmann (NF) [3], is the analog in smectic elastomers of the Helfrich-Hurault effect in uncrosslinked smectics [4,5]. Moreover, similar to thermotropic chiral smectics, chiral Sm*A* elastomers exhibit electrostriction, as depicted in Fig. 1, in which smectic layer spacing decreases in response to an electric field in the plane of the layers. Early experiments [6] produced a reduction in layer spacing by as much as 4% at field of 1.5 MV $m^{-1}$. More recent experiments [7] produce a reduction of 1% in fields as high as 3 MV $m^{-1}$ in films with one free edge to reduce mechanical stress. Even a 1% reduction in height is larger than that produced in most traditional actuators.

In this paper, we analyze the experiments just discussed using a phenomenological model of smectic elastomers we have recently developed [8,9]. This model, which generalizes the standard Lagrangian approach to elasticity theory [10,11], brings together in a single rubric physics associated with the crosslinked network that define the elastomer, the layering of the smectic phase, and the interaction between the nematic director and both the network and the smectic layers. It includes energies that favor constant smectic layer spacing and that lead to the development of shear strain in response to stretch perpendicular to layers above a critical stress. It also includes symmetry-permitted interactions between *c* ordering (molecular tilt relative to layer normal) and shear strain that cause shear to produce *c* ordering and vice versa. Thus a strain along the smectic layer normal produces the *c* ordering of a Sm*C* elastomer, as well as shear strain. We will analyze this instability of a Sm*A* elastomer under strain parallel to the layer normal in terms of an induced transition to a Sm*C* elastomer. Comparing our numerical estimates for the stress-strain behavior and the tilt of the smectic layers to the available experimental curves, we find convincing agreement. To analyze the electrostriction experiments, we add to our model the standard chiral couplings of the electric field to the Frank director and layer normal. The result is that an electric field in the plane of the

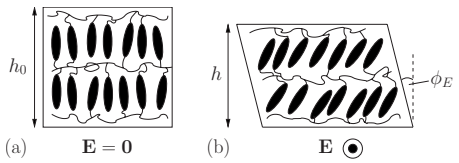


FIG. 1. Electroclinic effect in Sm$A^*$ elastomers. (a) Without electric field, the elastomeric film has a thickness $h_0$. (b) By application of a lateral electric field, a tilt angle $\phi_E$ is induced in a plane perpendicular to the field and the film thickness decreases to a value $h$.

*Present address: Department of Physics and Astronomy, University of Pennsylvania, Philadelphia, PA 19104, USA.

 

layers produces both Sm*C* ordering and shear strain linear in the electric field and a reduction in layer spacing quadratic in the field. Our numerical estimate of the magnitude of the reduction in layer spacing lies between the experimental values. To our knowledge, experiments have not sought to detect the shear strain induced by the external electric field.

Warner and Adams (AW) [12] have recently developed a theory of the elastic properties of Sm*A* elastomers that combines the neoclassical model of nematic elastomers [1] with the compressional energetics of smectic layers. This theory assumes that the nematic director is locked to the layer normal and that the elastomer is incompressible. Our theory is phenomenological; it is based on an expansion, consistent with all symmetries, of the free energy in powers of the Cauchy-Saint-Venant strain tensor [10] and the nematic director. The AW theory is semimicroscopic, and it applies, strictly speaking, solely to crosslinked networks of liquid crystal polymers. However, it provides a more realistic description of these particular elastomers than does our phenomenological model if strains are large. We compare the AW theory and ours in some detail, and we explain how the former theory can be extended to allow for relative tilt between the director and the layer normal. Though the details of the AW approach and ours us differ considerably, except for the development of Sm*C* order, they not surprisingly predict qualitatively identical results. A theory for chiral smectic elastomers was first set up by Terentjev and Warner [13,14] using group theory. Our theory with polarization generalizes the theory by Terentjev and Warner in a formalism that ensures invariance with respect to arbitrary rather than infinitesimal rotations of both the director and mass points.

The outline of our paper is as follows: Section II briefly reviews our model for smectic elastomers. Section III treats the behavior of Sm*A* elastomers under strain imposed along the layer normal. Exploiting the model reviewed in Sec. II, it derives predictions for the stress-strain behavior as well as the layer and the molecular tilt in response to strain. Section IV incorporates polarization into our model of Sec. II and considers the electroclinic effect and electrostriction. Section V presents concluding remarks. There is one Appendix that compares our theory in some detail to the AW theory as it stands. Moreover, the Appendix presents a generalization of the AW model that allows for Sm*C* ordering.

## II. MODELING SMECTIC ELASTOMERS

Let us first review briefly our model for smectic elastomers. Smectic elastomers are, as with any elastomer, permanently crosslinked amorphous solids whose static elasticity is most easily described in Lagrangian coordinates in which $\mathbf{x}$ labels a mass point in the undeformed (reference) material and $\mathbf{R}(\mathbf{x})=\mathbf{x}+\mathbf{u}(\mathbf{x})$, where $\mathbf{u}(\mathbf{x})$ is the displacement variable, labels the position of the mass point $\mathbf{x}$ in the deformed (target) material. Lagrangian elastic energies are formulated in terms of the strain tensor $\underline{\underline{u}}=\frac{1}{2}(\underline{\underline{g}}-\underline{\underline{\delta}})$ where $\underline{\underline{\delta}}$ is the unit matrix, $\underline{\underline{g}}=\underline{\underline{\Lambda}}^T\underline{\underline{\Lambda}}$ is the metric tensor, and $\Lambda_{ij}=\partial R_i/\partial x_j$ are the components of the Cauchy deformation tensor $\underline{\underline{\Lambda}}$ with $i,j,k=x,y,z$. The components of $\underline{\underline{u}}$ are thus $u_{ij}(\mathbf{x})=\frac{1}{2}(\Lambda^T_{ik}\Lambda_{kj}-\delta_{ij})=\frac{1}{2}(\partial_i u_j+\partial_j u_i+\partial_i u_k\partial_j u_k)$. Here and in the following the summation convention on repeated indices is understood.

As in nematic elastomers, the Frank director $\mathbf{n}$ interacts with the elastic strain. The strain $\underline{\underline{u}}$ is a reference-space tensor that transforms under the same reference-space operations that transform $\mathbf{x}$. The director $\mathbf{n}$, on the other hand, is a target-space vector that transforms under the same target-space operations that transform $\mathbf{R}$. To create scalar invariants coupling $\underline{\underline{u}}$ to $\mathbf{n}$, we need to convert $\mathbf{n}$ to a reference-state vector $\tilde{\mathbf{n}}$. This is accomplished with the aid of the polar decomposition [15] of the deformation tensor: $\underline{\underline{\Lambda}}=\underline{\underline{Q}}\underline{\underline{g}}^{1/2}$, where $\underline{\underline{g}}^{1/2}$ is a symmetric reference-space tensor and $\underline{\underline{Q}}=\underline{\underline{\Lambda}}\,\underline{\underline{g}}^{-1/2}$ is a rotation matrix. The components of $\underline{\underline{Q}}$ are $O_{ij}=\Lambda_{ik}[g^{-1/2}]_{kj}$, where we use the notation that $[M^\alpha]_{ij}$ is the $ij$ component of the matrix $\underline{\underline{M}}^\alpha$ for any square matrix $\underline{\underline{M}}$ and exponent $\alpha$ (it is understood that $M_{ij}\equiv[M]_{ij}$).

The left and right indices in $O_{ij}$ transform, respectively, under target- and reference-space operations, and $\underline{\underline{Q}}$ converts reference-space vectors to target-space vectors. Thus, we have $\mathbf{n}=\underline{\underline{Q}}\tilde{\mathbf{n}}$ and $\tilde{\mathbf{n}}=\underline{\underline{Q}}^T\mathbf{n}$. We will express the vectors $\mathbf{n}$ and $\tilde{\mathbf{n}}$ in terms of their components $c_a$ and $\tilde{c}_a$ perpendicular to the initial anisotropy axis along $z$: $n_i=c_a,n_z$ where $n_z=(1-c_a^2)^{1/2}\approx 1-\frac{1}{2}c_a^2$ and similarly for $\tilde{n}_i$, where we introduced the notation that letters $a,b,c,\ldots$, at the beginning of the alphabet run over the directions $x,y$ perpendicular to $z$. Reference-space vectors such as $\tilde{\boldsymbol{c}}$ and the vector $\tilde{\mathbf{e}}=(0,0,1)$ along the reference-space uniaxial direction [16] can be contracted with the strain $u_{ij}$ to produce scalars such as $\tilde{c}_a u_{ab}\tilde{c}_b$ and $\tilde{c}_a u_{az}$.

We can now construct free-energy densities, which we will simply call energies, for the various contributions to the total energy $f$ of a smectic elastomer. There is a contribution $f_{\rm net}$ to $f$ that is identical to the soft elastic energy of nematic elastomers including both the familiar terms quadratic in $u_{ij}$ and $\tilde{c}_a$. The characteristic energies scales in this free energy are set by the volume bulk modulus $B\sim 3\times 10^9$ Pa, the network shear modulus $\mu\sim 10^6$, and moduli that scale as $\mu$ times a factor that vanishes when the ratio $p$ of the polymer step lengths parallel and perpendicular to the local director becomes unity.

Smectic elastomers have a layer structure with a preferred layer spacing whose magnitude depends on the angle $\Theta$ between $\mathbf{n}$ and the layer normal $\mathbf{N}$ (or, equivalently, between $\tilde{\mathbf{n}}$ and $\tilde{\mathbf{N}}$). Smectic order is described by a complex mass-density-wave amplitude whose phase is $\phi=q_0[R_z-U(\mathbf{R})]=q_0\{z+u_z(\mathbf{x})-U[\mathbf{R}(\mathbf{x})]\}$, where $U(\mathbf{R})$ is the displacement field of the smectic layers, and $q_0=2\pi/d$, where $d$ is the preferred layer spacing when $\mathbf{n}$ is parallel to $\mathbf{N}$. We consider only elastomers crosslinked in the smectic phase in which case, $U[\mathbf{R}(\mathbf{x})]=u_z(\mathbf{x})$, and $\phi=q_0 z$. The energy associated with changes in the smectic layer spacing is

$$f_{\rm layer}=\frac{1}{2}B_{\rm sm}q_0^{-4}[(\mathbf{n}\cdot\boldsymbol{\nabla}\phi)^2-q_0^2]^2, \tag{2.1}$$

where $B_{\rm sm}$ is the smectic compression modulus with a value of order $10^7$ Pa deep in the smectic phase though it vanishes as the nematic phase is approached. $f_{\rm layer}$ favors a layer spac-

TABLE I. Contributions to coefficients in $f$ from $f_{\rm net}$, $f_{\rm layer}$, and $f_{\rm tilt}$ with $a=\mu(p-1)^2/(2p)$.

| | $C_1$ | $C_2$ | $C_3$ | $C_4$ | $C_5$ | $B_1$ | $B_2$ | $\lambda_1$ | $\lambda_2$ | $\lambda_3$ | $\lambda_4$ | $\lambda_5$ | $r$ | $v$ |
|---|---|---|---|---|---|---|---|---|---|---|---|---|---|---|
| net | $3\mu$ | $-\mu$ | $4B-\mu$ | $\mu$ | $\frac{1}{2}\mu\frac{(p+1)^2}{p}$ | $a$ | $-a$ | $\mu\frac{2p^2-p-1}{2p}$ | $-\mu\frac{p-1}{2p}$ | $-\mu\frac{p-1}{p}$ | $-\mu\frac{p^2-1}{p}$ | $-\frac{3}{2}a$ | $2a$ | 0 |
| layer | $4B_{\rm sm}$ | 0 | 0 | 0 | 0 | $6B_{\rm sm}$ | $\frac{9}{2}B_{\rm sm}$ | $2B_{\rm sm}$ | 0 | 0 | 0 | $4B_{\rm sm}$ | 0 | $2B_{\rm sm}$ |
| tilt | 0 | 0 | 0 | 0 | $\frac{1}{2}r_t$ | $\frac{1}{2}r_t$ | $\frac{1}{2}r_t+\frac{1}{4}v_t$ | 0 | 0 | 0 | $r_t$ | $-\frac{1}{2}r_t$ | $r_t$ | $v_t$ |

ing of $d'=d/\cos\Theta$, where as before $\Theta$ is the angle between $\mathbf{n}$ and $\mathbf{N}$.

Finally, there are interactions favoring $\tilde{\mathbf{n}}$ parallel to $\tilde{\mathbf{N}}$ in the smectic-*A* phase and tilted relative to $\tilde{\mathbf{N}}$ in the smectic-*C* phase:

$$f_{\rm tilt}=\frac{1}{2}r_t\sin^2\Theta+\frac{1}{4}v_t\sin^4\Theta. \tag{2.2}$$

The energy $f_{\rm layer}+f_{\rm tilt}$ is the generalization to smectic elastomers of the Chen-Lubensky model [17] for Sm*A*-Sm*C*-nematic phase behavior in uncrosslinked liquid crystals. Its coefficient $r_t$ is linear in the deviation of the temperature $T$ from the transition temperature $T_c$ between the Sm*A* and Sm*C* phases, $r_t=\alpha|T-T_c|$. The coefficient $v_t$ is essentially independent of temperature. Experiments by Brehmer, Zentel, Gießelmann, Germer, and Zungenmaier (BZGGZ) [18] on smectic elastomers measured the values of the coefficients of a tilt energy similar to our $f_{\rm tilt}$ (however, their tilt energy is somewhat more general in that it also accounts for polarization effects which we will discuss later). A short calculation translates their experimental values into estimates for our $\alpha$ and $v_t$: $\alpha\sim1.3\times10^4$ Pa/K and $v_t\sim5\times10^5$ Pa. At a temperature of 20 K above the transition temperature, $r_t$ is or order $10^5$ Pa. More recently, similar experiments were performed on liquid smectics by Archer and Dierking (AD) [19]. Their results lead to $\alpha\sim4\times10^4$ Pa/K and $v_t\sim10^6$ Pa implying that $r_t\sim10^6$ Pa at 20 K above the transition temperature. Though measured for liquid smectics, the AD values should be of some relevance to elastomeric smectics, and we will use them in the following in addition to the BZGGZ values in order to put the estimates that we are going to make on a broader basis.

The energy of a smectic elastomer $f=f_{\rm net}+f_{\rm layer}+f_{\rm tilt}$ can now be expressed as a sum of a harmonic uniaxial elastic contribution $f_{\rm uni}$ depending only on $u_{ij}$, a contribution $f_{\rm nonlin}$ depending only on $u_{ij}$ that collects the relevant nonlinear terms, a contribution $f_c$ describing the energy associated with the formation of nonvanishing $c$ order described by $\tilde{c}_a$, and a contribution $f_{\rm coupl}$ arising from the coupling of $u_{ij}$ and $\tilde{c}_a$:

$$f=f_{\rm uni}+f_{\rm nonlin}+f_c+f_{\rm coupl}. \tag{2.3}$$

The uniaxial elastic energy to harmonic order in strains is

$$f_{\rm uni}=\tfrac{1}{2}C_1u_{zz}^2+C_2u_{zz}u_{ii}+\tfrac{1}{2}C_3u_{ii}^2+C_4\hat{u}_{ab}^2+C_5u_{az}^2, \tag{2.4}$$

where

$$\hat{u}_{ab}=u_{ab}-\tfrac{1}{2}\delta_{ab}u_{cc} \tag{2.5}$$

is the two-dimensional symmetric, traceless strain tensor. The nonlinear energy reads

$$f_{\rm nonlin}=-B_1u_{zz}u_{az}^2+B_2(u_{az}^2)^2. \tag{2.6}$$

The $c$-director energy is

$$f_c=\tfrac{1}{2}r\tilde{c}_a^2+\tfrac{1}{4}v(\tilde{c}_a^2)^2, \tag{2.7}$$

and the coupling energy is

$$f_{\rm coupl}=\lambda_1\tilde{c}_a^2u_{zz}+\lambda_2\tilde{c}_a^2u_{ii}+\lambda_3\tilde{c}_a\hat{u}_{ab}\tilde{c}_b+\lambda_4\tilde{c}_au_{az}+\lambda_5u_{zz}\tilde{c}_au_{az}. \tag{2.8}$$

Table I reviews the relations between the original elastic constants of $f_{\rm net}$, $f_{\rm layer}$, and $f_{\rm tilt}$ and the effective elastic constants featured in Eq. (2.4) and Eqs. (2.6)–(2.8). As mentioned earlier, the parameter $p$ appearing in Table I is the anisotropy ratio. In the work of NF, the samples showed at the transition temperature a spontaneous stretch along the director of about 12%. When making estimates, we will view $p\approx1.1$ as a typical value. Based on the relations given in Table I, we deduce that the hierarchy of magnitudes of the effective elastic constants is $C_3\sim10^9$ Pa, $C_1\sim B_1\sim B_2\sim v\sim\lambda_1\sim\lambda_5\sim10^7$ Pa, $C_2\sim C_4\sim C_5\sim r\sim\mu\sim10^6$ Pa, $\lambda_3\sim-10^5$ Pa, and $\lambda_2\sim-10^4$ Pa. Our estimates for $r$ and $\lambda_4$ depend noticeably on whether we use the BZGGZ or the AD values: we expect $r\sim10^5$ Pa and $\lambda_4\sim-10^5$ Pa based on BZGGZ and $r\sim\lambda_4\sim10^6$ Pa based on AD. It is worth commenting on the sign of $\lambda_4$. Our estimates of its value have different signs for the two physical systems for which we have data. This is possible because the two contributions to $\lambda_4$ have opposite signs. The second contribution $r_t$, which is positive, arises because $\Theta\approx\tilde{c}_a+u_{az}$, and the $\frac{1}{2}r_t\sin^2\Theta$ term favors $\tilde{c}_a=-u_{az}$. The first term, $-\mu(p^2-1)/p$, describes the rotation of $\tilde{c}_a$ in response to the imposition of a shear $u_{az}$. It is negative and it favors a $\tilde{c}_a$ with the same sign as $u_{az}$.

Several observations about $f$ are in order. First, $\tilde{c}_a$ and $u_{az}$ are coupled at linear order via the $\lambda_4$ term. Thus, if a nonzero $u_{az}$ develops, it will be accompanied by the development of a nonzero $\tilde{c}_a$ and vice versa. Negative $\lambda_4$ favors mechanical tilt and mesogenic tilt in the same direction whereas positive $\lambda_4$ favors opposite tilt directions. If, for example, $u_{zz}=0$ and $u_{az}\neq0$, then $\tilde{c}_a$ relaxes to $\tilde{c}_a=-(\lambda_4/r)u_{az}$ to minimize $f$. This leads to and effective or renormalized value of the shear modulus $C_5$,

$$C_5^R=C_5-\frac{\lambda_4^2}{2r}. \tag{2.9}$$

If, to give another example, $u_{zz}=0$ and $\tilde{c}_a\neq0$, $u_{az}$ relaxes to $u_{az}=-\lambda_4/(2C_5)\tilde{c}_a$ and $r$ is renormalized to $r_R=r-\lambda_4^2/(2C_5)$. Note that the value of the renormalized elastic constants $C_5^R$ and $r_R$ does not depend on the sign of $\lambda_4$. Second, an externally imposed strain $u_{zz}$ reduces the coefficient of $u_{az}^2$ via the

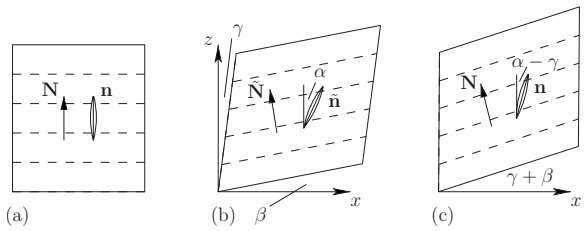


FIG. 2. Schematic representation of distortions in the $xz$ plane induced by the Sm$A$-to-Sm$C$ transition: (a) undistorted Sm$A$ phase, (b) Sm$C$ phase with a symmetric deformation tensor $\underline{\underline{\Lambda}}_S$, and (c) Sm$C$ phase with $\Lambda_{xz}=0$ and $\Lambda_{zx}>0$.

$B_1$ term. This leads to the elastomer version of the Helfrich-Hurault [4,5] instability, which we will discuss in Sec. III. Finally, if $\tilde{c}_a$ becomes nonzero, there will be an accompanying decrease in $u_{zz}$ and the smectic layer spacing proportional to $\tilde{c}_a^2$ via the $\tilde{c}_a^2 u_{zz}$ term with positive coupling constant $\lambda_1$. The reduction of layer spacing in response to an external electric field that tilts the director in chiral systems will be the subject of Sec. IV

## III. ELASTICITY OF SMECTIC-$A$ ELASTOMERS UNDER STRAIN IMPOSED ALONG THE LAYER NORMAL

Before we start with our analysis, it is useful to clarify the experimental conditions. In the experiments of NF [3], the Sm$A$ sample is subjected to an external uniaxial stress normal to the smectic layers. This stress stretches the sample, producing a deformation tensor $\underline{\underline{\Lambda}}$ with $\Lambda_{zz}>1$. If there is a transition to the Sm$C$ phase, the sample will undergo a shape change, as sketched in Fig. 2, from a rectangular parallelepiped to a nonrectangular one with two parallel nonrectangular faces. The external stress is applied along the space-fixed $z$ axis and causes the target space vector $\mathbf{R}$ to stretch along the $z$ axis. This defines a preferred orientation in the target space and therefore breaks rotational invariance in this space. In an idealized experiment, the external stress will stretch the sample parallel to the $z$ axis in the target space only, regardless of the shape of the nonrectangular faces. Thus, in the Sm$C$ phase, the configuration of the sample will be that [shown in Fig. 2(c)] of a simple shear in which $\Lambda_{zx}>0$ and $\Lambda_{xz}=0$. In a real experiment, boundary conditions prevent a distortion with a spatially uniform value of $\Lambda_{zx}$, and the system breaks up into oppositely tilted domains. We will ignore this effect in our analysis. Thus, the general form for the deformation tensor under uniaxial stress along the target-space $z$ axis is

$$\underline{\underline{\Lambda}} = \begin{pmatrix} \Lambda_{xx} & 0 & 0 \\ 0 & \Lambda_{yy} & 0 \\ \Lambda_{zx} & 0 & \Lambda_{zz} \end{pmatrix}, \tag{3.1}$$

where $\Lambda_{zx}=0$ in the Sm$A$ phase. This then implies a strain tensor

$$\underline{\underline{u}} = \frac{1}{2}\begin{pmatrix} \Lambda_{xx}^2 + \Lambda_{zx}^2 - 1 & 0 & \Lambda_{zx}\Lambda_{zz} \\ 0 & \Lambda_{yy}^2 - 1 & 0 \\ \Lambda_{zx}\Lambda_{zz} & 0 & \Lambda_{zz}^2 - 1 \end{pmatrix}. \tag{3.2}$$

Thus, the $zz$ component of the strain tensor, $u_{zz}=(\Lambda_{zz}^2-1)/2$, depends only on the imposed strain deformation $\Lambda_{zz}$ in both phases. The formation of the Sm$C$ phase is signalled by the development of a nonzero shear strain $u_{xz}=\Lambda_{zx}\Lambda_{zz}/2$.

As we indicated earlier, the imposition of a sufficiently large positive strain $u_{zz}$ induces a transition to a new phase with a nonvanishing shear strain $u_{az}$. Because of the linear coupling $\lambda_4 \tilde{c}_a u_{az}$ between strain and $c$ director in $f_{\text{coupl}}$, director tilt develops along with shear strain, and the phase with nonzero $u_{az}$ can be viewed as a strain-induced Sm$C$ phase. Effective energies in terms of either $u_{az}$ or $\tilde{c}_a$ provide equally valid descriptions of the transition. Here we will describe the transition in terms of an effective energy expressed in terms of $\tilde{c}_a$. To arrive at this energy, we must relax the variables $u_{ii}$, $\hat{u}_{ab}$, and $u_{az}$ to their equilibrium values in the presence of nonvanishing $\tilde{c}_a$ and $u_{zz}$. The equations for $\partial f/\partial u_{ii}=0$ and $\partial f/\partial \hat{u}_{ab}=0$ are linear and are easily solved for $u_{ii}$ and $\hat{u}_{ab}$:

$$u_{ii} = -\frac{C_2}{C_3}u_{zz} - \tau \tilde{c}_a^2, \tag{3.3a}$$

$$\hat{u}_{ab} = -\omega\left(\tilde{c}_a\tilde{c}_b - \tfrac{1}{2}\delta_{ab}\tilde{c}_c^2\right), \tag{3.3b}$$

where

$$\tau = \lambda_2/C_3 \quad \text{and} \quad \omega = \lambda_3/(2C_4). \tag{3.4}$$

The equation of state for $u_{az}$ is nonlinear:

$$\frac{\partial f}{\partial u_{az}} = 2C_5(u_{zz})u_{ab} + 4B_2 u_{bz}^2 u_{az} + \lambda_4(u_{zz})\tilde{c}_a, \tag{3.5}$$

where

$$C_5(u_{zz}) = C_5 - B_1 u_{zz}, \tag{3.6a}$$

$$\lambda_4(u_{zz}) = \lambda_4 + \lambda_5 u_{zz}. \tag{3.6b}$$

Since we are interested in properties near the transition, we solve Eq. (3.5) for $u_{az}$ to third-order in $\tilde{c}_a$:

$$u_{az} = -\rho(u_{zz})\tilde{c}_a + 2B_2\frac{\rho^3(u_{zz})}{C_5(u_{zz})}\tilde{c}_b^2\tilde{c}_a, \tag{3.7}$$

where

$$\rho(u_{zz}) = \frac{\lambda_4(u_{zz})}{2C_5(u_{zz})}. \tag{3.8}$$

Inserting Eqs. (3.3a), (3.3b), and (3.7) into the free energy of Eq. (2.3), we obtain an effective energy expressed as a function of $\tilde{c}_a$ and $u_{zz}$ (the latter being fix externally),

$$f_{\text{eff}} = \tfrac{1}{2}C_1^R u_{zz}^2 + \tfrac{1}{2}r_R(u_{zz})\tilde{c}_a^2 + \tfrac{1}{4}v_R(u_{zz})\tilde{c}_a^2\tilde{c}_b^2, \tag{3.9}$$

where

$$C_1^R = C_1 - C_2^2/C_3, \tag{3.10a}$$

$$r_R(u_{zz}) = r + 2(\lambda_1 - C_2\tau)u_{zz} - 2C_5(u_{zz})\rho^2(u_{zz}), \tag{3.10b}$$

$$v_R(u_{zz}) = v - 2C_4\omega^2 - 2C_3\tau^2 + 4B_2\rho^4(u_{zz}). \tag{3.10c}$$

We can now use $f_{\text{eff}}$ to analyze the transition to the Sm$C$ phase induced by the uniaxial strain $u_{zz}$. The term $2C_5(u_{zz})\rho^2(u_{zz})=\lambda_4^2(u_{zz})/2C_5(u_{zz})$ in $r_R(u_{zz})$ diverges at $u_{zz}=C_5/B_1$ and guarantees that $r_R(u_{zz})$ will pass through zero upon increasing $u_{zz}$. $u_{zz}^c$, the critical value of $u_{zz}$ at which $r_R=0$, is given by

$$u_{zz}^c = \Delta^{-1}[\Xi - \sqrt{\Xi^2 - 2rC_5^R\Delta}], \tag{3.11}$$

with $C_5^R$ as given in Eq. (2.9), and where $\Delta=4B_1(\tau C_2-\lambda_1)-\lambda_5^2$ and $\Xi=rB_1+2\tau C_2C_5-2C_5\lambda_1+\lambda_4\lambda_5$. Both, the BZGGZ and the AD values lead to $u_{zz}^c\approx 0.03$ in good agreement with the experimental estimate of 0.034 [3]. In the vicinity of the critical point determined by $u_{zz}^c$, we can expand $r_R(u_{zz})$ and $g_R(u_{zz})$ to lowest order in $\delta u_{zz}=u_{zz}-u_{zz}^c$:

$$r_R(u_{zz}) = -b\,\delta u_{zz}, \tag{3.12a}$$

$$v_R(u_{zz}) = v_R(u_{zz}^c) \equiv v_R^c, \tag{3.12b}$$

where $b=-\partial r_R(u_{zz})/\partial u_{zz}|_{u_{zz}=u_{zz}^c}>0$. Choosing our coordinate system so that the $c$ director induced by the $u_{zz}$ strain lies along the $x$ direction we obtain $\tilde{c}_y^0=0$ and

$$\tilde{c}_x^0 = \begin{cases} 0 & \text{for } u_{zz} < u_{zz}^c, \\ \pm s\sqrt{\delta u_{zz}} & \text{for } u_{zz} > u_{zz}^c, \end{cases} \tag{3.13}$$

where $s=\sqrt{b/v_R^c}$. The director in the Sm$C$ phase under a symmetric shear, i.e., in the geometry shown in Fig. 2(b), is therefore $\tilde{\mathbf{n}}=(\sin\alpha,0,\cos\alpha)$, where $\sin\alpha=\tilde{c}_x^0$. Using the BZGGZ and the AD values, we estimate $s\approx 0.75$ and 0.8, respectively.

From the equilibrium values of the $c$-director, it is a straightforward exercise to determine the equilibrium strain tensor $\underline{\underline{u}}^0$ from Eqs. (3.3a), (3.3b), and (3.7). Consistent with Eq. (3.2), there is no shear induced by $u_{zz}$ in the $xy$ plane, $u_{xy}^0=0$, and there is no shear induced in the $yz$ plane, $u_{yz}^0=0$. There is, however, a shear in the $xz$ plane, which according to Eqs. (3.7) and (3.13) is

$$u_{xz}^0 = \begin{cases} 0 & \text{for } u_{zz} < u_{zz}^c, \\ \mp\rho_c s\sqrt{\delta u_{zz}} & \text{for } u_{zz} > u_{zz}^c, \end{cases} \tag{3.14}$$

to lowest order in $\delta u_{zz}$ with $\rho_c\equiv\rho(u_{zz}^c)$. The BZGGZ and AD values, respectively, lead to $\rho_c\approx 1.2$ and 1.1.

The equilibrium values for extensional strains follow from Eqs. (3.3a), (3.3b) and $u_{ii}=u_{aa}+u_{zz}$. To lowest order in $\delta u_{zz}$,

$$u_{xx}^0 = -\frac{1}{2}\left[1 + \frac{C_2}{C_3}\right]u_{zz} \quad \text{for } u_{zz} < u_{zz}^c, \tag{3.15a}$$

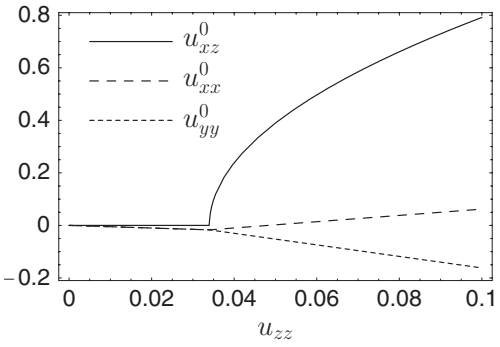


FIG. 3. Dependence (schematic) of the nonzero equilibrium strain components on $u_{zz}$.

$$u_{xx}^0 = -\frac{1}{2}\left[1 + \frac{C_2}{C_3}\right]u_{zz}^c - \frac{1}{2}\left[1 + \frac{C_2}{C_3} + (\tau+\omega)a^2\right]\delta u_{zz} \quad \text{for } u_{zz} < u_{zz}^c, \tag{3.15b}$$

and $u_{yy}^0$ is given by Eq. (3.15) with $\omega$ replaced by $-\omega$. The parameter $\omega=\lambda_3/(2C_5)=-[\mu(p-1)/p][r_t+\mu(p-1)^2/p]$ is negative and of order $-0.05$. Figure 3 depicts the equilibrium strain components on $u_{zz}$ schematically.

The quantities $\tilde{c}_x^0$ and $u_{xz}^0$ determine the equilibrium angle $\Theta^0$ between the layer normal and the director. To lowest order,

$$\Theta^0 = \tilde{c}_x^0 + u_{xz}^0 = [1-\rho_c]\tilde{c}_x^0. \tag{3.16}$$

The coefficient $1-\rho_c$ of $\tilde{c}_x^0$ on the right hand side is negative and of the order of $-0.2$ or $-0.1$, depending on whether we use the BZGGZ or the AD values. The small but nonzero $1-\rho_c$ implies that the tilt angles of the layer normal and the director are distinct and that, however, their difference will be small for $u_{zz}$ not too far above $u_{zz}^c$. We will revisit the tilt angles of the layer normal and the director further below.

Now we turn to the effective elastic energy density as a function of $u_{zz}$ only when the other strain components and $\tilde{\mathbf{c}}$ have relaxed to their equilibrium values. Plugging $\tilde{c}_a^0$, into Eq. (3.9), we obtain to quadratic order in $u_{zz}$

$$f = \frac{1}{2}C_1^R u_{zz}^2 \quad \text{for } u_{zz} < u_{zz}^c \tag{3.17a}$$

and

$$f = \frac{1}{2}C_1^R(u_{zz}^c + \delta u_{zz})^2 - \frac{1}{2}D_1(\delta u_{zz})^2 \quad \text{for } u_{zz} > u_{zz}^c, \tag{3.17b}$$

where $D_1=(1/2)b^2/v_R^c$. Note that the two branches (3.17a) and (3.17b) match at $u_{zz}^c$ as they should.

Next, we address the relation between stress and strain. The engineering or first Piola-Kirchhoff stress measured in experiments is $\sigma_{ij}^{\text{eng}}=\Lambda_{ik}\sigma_{kj}$, where $\sigma_{kj}=\partial f/\partial u_{kj}$ is the symmetric second Piola-Kirchhoff stress tensor. The system reaches equilibrium at fixed $u_{zz}$ with respect to all other components of $u_{ij}$, i.e., $\sigma_{ij}=0$ for $ij\neq zz$. Thus, the $zz$ component of the engineering stress tensor is $\Lambda_{zz}\sigma_{zz}$ and

$$\sigma_{zz}^{\text{eng}} = C_1^R \Lambda_{zz} u_{zz} \quad \text{for } u_{zz} < u_{zz}^c \tag{3.18a}$$

and

$$\sigma_{zz}^{\text{eng}} = C_1^R u_{zz}^c \Lambda_{zz} + [C_1^R - D_1]\Lambda_{zz}\delta u_{zz} \quad \text{for } u_{zz} > u_{zz}^c. \tag{3.18b}$$

For the deformation tensor of Eq. (3.1) and small strain, $\Lambda_{zz} = \sqrt{1+2u_{zz}} \approx 1+u_{zz}$. Thus, if the critical strain $u_{zz}^c$ is small as our estimates indicate

$$\sigma_{zz}^{\text{eng}} \approx C_1^R u_{zz} \quad \text{for } u_{zz} < u_{zz}^c. \tag{3.19a}$$

For $u_{zz} > u_{zz}^c$ and small $\delta u_{zz}$,

$$\sigma_{zz}^{\text{eng}} \approx C_1^R u_{zz}^c + [C_1^R - D_1]\delta u_{zz} \quad \text{for } u_{zz} > u_{zz}^c, \tag{3.19b}$$

provided that $C_1^R \neq D_1$, and hence the Young's modulus $Y_\parallel$ is given by

$$Y_\parallel = \begin{cases} C_1^R & \text{for } u_{zz} < u_{zz}^c, \\ C_1^R - D_1 & \text{for } u_{zz} > u_{zz}^c, \end{cases} \tag{3.20}$$

in this case. Adams and Warner in fact find $C_1^R = D_1$ in their model, and we obtain the same result in our treatment if we lock $\mathbf{n}$ to $\mathbf{N}$ and set $f = f_{\text{net}} + f_{\text{layer}}$. This limit does not follow cleanly from the model in Eq. (2.3) and the parameters of Table I because that model does not include all of the fourth-order terms in the free energy of the original model defined $f = f_{\text{net}} + f_{\text{layer}} + f_{\text{tilt}}$. If $C_1^R = D_1$, then $\sigma_{zz}^{\text{eng}} = C_1^R u_{zz}^c \Lambda_{zz}$ so that the leading terms for $u_{zz}^c \ll \delta u_{zz} \ll 1$ are

$$\sigma_{zz}^{\text{eng}} \approx C_1^R u_{zz}^c + C_1^R u_{zz}^c \delta u_{zz} \quad \text{for } u_{zz} > u_{zz}^c, \tag{3.21}$$

implying that

$$Y_\parallel = \begin{cases} C_1^R & \text{for } u_{zz} < u_{zz}^c, \\ C_1^R u_{zz}^c & \text{for } u_{zz} > u_{zz}^c, \end{cases} \tag{3.22}$$

if $C_1^R = D_1$. Equations (3.19) and (3.21) reveal that $\sigma_{zz}^{\text{eng}}$ as a function of $u_{zz}$ will consist of two straight lines of different slope (Young's modulus) meeting at $u_{zz} = u_{zz}^c$. If $C_1^R = D_1$, then the ratio of the Young's modulus for $u_{zz} > u_{zz}^c$ to that for $u_{zz} < u_{zz}^c$ is simply $u_{zz}^c$. Our full equations (3.18) show that there are nonlinear corrections to $\sigma_{zz}^{\text{eng}}$ both above and below $u_{zz}^c$. Since the experimental value of $u_{zz}^c \approx 0.034$ is much less than one, the nonlinear corrections below $u_{zz}^c$ are unimportant. Those above $u_{zz}^c$ vanish or are unimportant if $C_1^R$ and $D_1$ are equal or nearly so. Figure 4 shows the linearized stress-strain behavior along with experimental data. Both, Eqs. (3.19b) and (3.21) are used in the plots and both produce excellent agreement with the experimental data.

For completeness we note that, if we use our strain-only model for the Sm*A*-to-Sm*C* transition [8], we find, to leading order in $\delta u_{zz}$, essentially the same equilibrium strain tensor, the same effective elastic energy, and the same stress-strain relation as AW. Obvious differences reside in the different definitions of the elastic constants used in both models. These differences are of course qualitatively unimportant.

Next we calculate the tilt angle $\varphi$ of the layer normal in response to $u_{zz}$. As illustrated in Fig. 2, the angle that $\mathbf{N}$ makes with the $z$ axis is

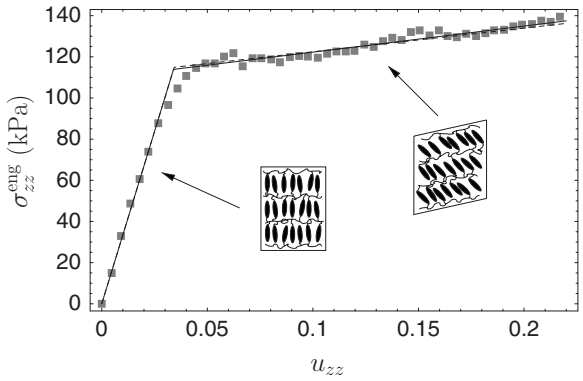


FIG. 4. The engineering stress $\sigma_{zz}^{\text{eng}}$ as a function of strain $u_{zz}$ of a monodomain Sm*A* elastomer. The squares symbolize experimental data by Nishikawa and Finkelmann [3]. Above a threshold strain of about 3% the elastomer is in a Sm*C*-like phase with an elastic modulus much lower than that of the original Sm*A* phase below the threshold. The continuous lines stem from Eqs. (3.19a) and (3.19b) with $u_{zz}^c = 0.034$, $C_1^R = 3.5 \times 10^7$ Pa, and $D_1 = 3.223 \times 10^7$ Pa. The dashed lines stem from Eqs. (3.19a) and (3.21) with $u_{zz}^c = 0.0343$ and $C_1^R = 3.5 \times 10^7$ Pa. The continuous and dashed lines lie almost on top of each other and are therefore hard to distinguish.

$$\varphi = \beta + \gamma, \tag{3.23}$$

where $\beta$ is the angle that $\tilde{\mathbf{N}}$ makes with the $z$ axis and $\gamma$ is the clockwise angle about the $y$ axis through which the sample under symmetric shear has to be rotated to bring it into the configuration with $\Lambda_{xz} = 0$. In terms of the components of the symmetric deformation tensor $\underline{\underline{\Lambda}}_S$, these angles are given by

$$\beta = \tan^{-1}\left(\frac{\Lambda_{Szx}^0}{\Lambda_{Sxx}^0}\right) \approx \frac{u_{xz}^0}{1 - \frac{1}{2}(1 + C_2/C_3)u_{zz}^c}, \tag{3.24a}$$

$$\gamma = \tan^{-1}\left(\frac{\Lambda_{Szx}^0}{\Lambda_{Szz}}\right) \approx \frac{u_{xz}^0}{1 + u_{zz}^c}. \tag{3.24b}$$

We find that $\varphi$ vanishes as $\delta u_{zz} \to 0$, and near $\delta u_{zz} = 0$, its expansion to order $(\delta u_{zz})^{3/2}$ is

$$\varphi = \begin{cases} 0 & \text{for } u_{zz} < u_{zz}^c, \\ A_1(\delta u_{zz})^{1/2} + A_3(\delta u_{zz})^{3/2} & \text{for } u_{zz} > u_{zz}^c. \end{cases} \tag{3.25}$$

The value of $A_1$ is determined entirely by the lowest order expressions for $u_{xz}^0$ [Eq. (3.14)] and $u_{xx}^0$ [Eq. (3.15)],

$$A_1 = s\rho_c \frac{2 + \frac{1}{2}(1 - C_2/C_3)u_{zz}^c}{[1 + u_{zz}^c]\left[1 - \frac{1}{2}(1 + C_2/C_3)u_{zz}^c\right]}. \tag{3.26}$$

$A_3$ has contributions both from the expansions of $\tan^{-1}$ to third order in its arguments, and from $(\delta u_{zz})^{3/2}$ contributions to $u_{xz}^0$ and $u_{xx}^0$, which we have not calculated. Both, the BZGGZ and AD values, lead to $A_1 \approx 1.8$. Next, we compare our result (3.25) and our estimate for $A_1$ with the experimental data by NF, see Fig. 5. For this comparison it is important to note that the expansion (3.25) with $A_1$ given by Eq. (3.26) expresses $\varphi$ in its natural unit, radian. The experimental curve by NF as shown Fig. 5, on the other hand, measures $\varphi$

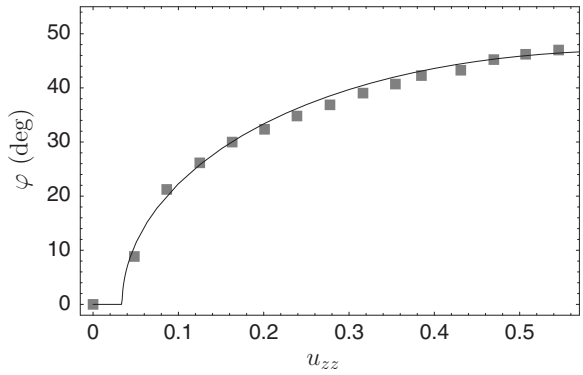


FIG. 5. Dependence of the tilt angle $\varphi$ on $u_{zz}$. The squares symbolize data taken from Ref. [3]. The continuous curve corresponds to our analytic result (3.25).

in degrees. Converting the above estimate for $A_1$ from radian to degrees we get the estimate $A_1 \approx 1.8 \times 360/(2\pi) \approx 100$. Fitting our result (3.25) to the experimental curve, we obtain $u_{zz}^c = 0.034$, $A_1 = 90$, and $A_3 = -49$. The fitted analytical and the experimental curve agree remarkably well, and the best-fit value $A_1 = 90$ is certainly of the same order of magnitude as our estimate $A_1 \approx 100$.

Finally, we calculate the tilt angle $\varphi_{\mathbf{n}}$ of the mesogens in response to $u_{zz}$. The angle that the target-space director makes with the $z$ axis is, as depicted in Fig. 2,

$$\varphi_{\mathbf{n}} = \alpha - \gamma, \tag{3.27}$$

where $\alpha = \sin^{-1} \tilde{c}_x^0$. Similar to $\varphi$, $\varphi_{\mathbf{n}}$ vanishes as $\delta u_{zz} \to 0$. In the vicinity of $\delta u_{zz} = 0$, its expansion to order $(\delta u_{zz})^{3/2}$ is

$$\varphi_{\mathbf{n}} = \begin{cases} 0 & \text{for } u_{zz} < u_{zz}^c, \\ A_{\mathbf{n},1}(\delta u_{zz})^{1/2} + A_{\mathbf{n},3}(\delta u_{zz})^{3/2} & \text{for } u_{zz} > u_{zz}^c, \end{cases} \tag{3.28}$$

with the value of $A_{\mathbf{n},1}$ being determined entirely by the lowest order expressions for $\tilde{c}_x^0$ [Eq. (3.13)] and $u_{xz}^0$ [Eq. (3.14)],

$$A_{\mathbf{n},1} = s + \frac{s\rho_c}{1 + u_{zz}^c}. \tag{3.29}$$

$A_{\mathbf{n},3}$ has contributions both from the expansions of $\sin^{-1}$ and $\tan^{-1}$ to third order in their arguments, and from $(\delta u_{zz})^{3/2}$ contributions to $\tilde{c}_x^0$ and $u_{xz}^0$, which we have not calculated. From the BZGGZ and AD values we obtain, respectively, approximately $A_{\mathbf{n},1} \approx 85$ and $A_{\mathbf{n},1} \approx 90$ when $\varphi_{\mathbf{n}}$ is measured in degrees.

In their experiments, NF did not seek to produce curves of $\varphi_{\mathbf{n}}$ versus $u_{zz}$. From measuring the layer thickness as a function of $u_{zz}$ and by interpreting their x-ray reflection patterns, however, they conclude that the layer normal and the director remain parallel above the threshold strain and that the reduction of $Y_{\parallel}$ above the threshold stems form a strain induced breakdown of the smectic layers into pieces with local Sm*A* order. Our theory, on the other hand, predicts that the angles $\varphi$ and $\varphi_{\mathbf{n}}$ are different but of the same order of magnitude, and that the reduction of $Y_{\parallel}$ results from shear and Sm*C*-like ordering produced by sample extension. If the difference between $\varphi$ and $\varphi_{\mathbf{n}}$ is small, it can be difficult to distinguish between Sm*A* and Sm*C* order experimentally. If this is the case in the experiments of NF, then the differences between the experimental findings and our theoretical predictions for the tilt angles may lie within the experimental error.

Above, we have at several occasions briefly commented on the relation of our work to that of AW. A more detailed comparison of the two approaches can be found in the Appendix .

## IV. ELECTROCLINIC EFFECT IN SM$A^*$ ELASTOMERS

In a chiral smectic elastomer an external electric field $\mathbf{E}$ can couple to both the elastic and the orientational degrees of freedom. First, we consider the former coupling. $\mathbf{E}$, like the director $\mathbf{n}$ and the layer normal $\mathbf{N}$, is a vector in the target space and hence cannot be coupled directly to the reference space tensor $\underline{\underline{u}}$. By now, of course, we know how to overcome this problem: we can use the polar decomposition theorem to switch from $\mathbf{E}$ to its reference space counterpart $\tilde{\mathbf{E}}$ via the transformation $\tilde{\mathbf{E}} = \underline{\underline{Q}}^T \mathbf{E}$ and then construct form $\tilde{\mathbf{E}}$ and $\underline{\underline{u}}$ couplings that are manifestly invariant under simultaneous rotations of the sample and the field in the reference space. Since we are interested in Sm$A^*$ elastomers, the couplings have to conform with uniaxial symmetry in the reference space which leads us to

$$f_{E,1} = -v_1 \tilde{E}_a \hat{u}_{ab} \tilde{E}_b - v_2 u_{zz} \tilde{E}_z^2, \tag{4.1}$$

where $v_1$ and $v_2$ are coupling constants. In Eq. (4.1) we have omitted a term of the type $u_{aa}\tilde{E}_b^2$ to keep our discussion as simple as possible. This omission does not affect our results qualitatively.

Now we come to the coupling between the electric field and the orientational degrees of freedom. In a chiral smectic a spontaneous polarization $\mathbf{P}$ occurs if the director $\mathbf{n}$ and the layer normal $\mathbf{N}$ are neither parallel nor perpendicular:

$$\mathbf{P} \sim \mathbf{n} \times \mathbf{N}(\mathbf{n} \cdot \mathbf{N}). \tag{4.2}$$

Thus, in the presence of $\mathbf{E}$, the elastic energy density of the elastomer has an extra contribution

$$f_{E,2} \sim \mathbf{E} \cdot \mathbf{n} \times \mathbf{N}(\mathbf{n} \cdot \mathbf{N}). \tag{4.3}$$

In order to combine $f_{E,2}$ with the remaining terms of the elastic energy density we recast $f_{E,2}$ in the reference space to obtain

$$f_{E,2} = K\tilde{\mathbf{E}} \cdot \tilde{\mathbf{n}} \times \tilde{\mathbf{N}}(\tilde{\mathbf{n}} \cdot \tilde{\mathbf{N}}), \tag{4.4}$$

where $K$ is a coupling constant. The experimental findings by BZGGZ imply $K \sim 10^{-3}$ Pa(m/V), whereas the value of $K$ implied in the results by AD is one order of magnitude smaller, $K \sim 10^{-4}$ Pa(m/V).

In the typical experimental setup, the normal of the elastomeric film is along the $z$ direction and the electric field $\mathbf{E}$ is along the $y$ direction. If we assume that the experiments correspond to the geometry shown in Fig. 1, then $\Lambda_{zx}^0 = 0$ but $\Lambda_{xz}^0 \neq 0$, and the only nonzero components of $\underline{\underline{\Lambda}}$ are $\Lambda_{xx}^0$, $\Lambda_{yy}^0$, $\Lambda_{zz}^0$, and $\Lambda_{xz}^0$, implying that $O_{xy} = O_{yx} = O_{yz} = O_{zy} = 0$. Thus $\tilde{E}_i$

$=O_{ij}^T E_j = E_i$, and $\tilde{\mathbf{E}}=(0,E,0)$. In addition, $\tilde{N}_i = [g^{-1/2}]_{iz}[g^{-1}]_{zz}^{-1/2} \approx (-u_{az}, 1-\frac{1}{2}u_{az}^2)$. With these expressions, the above coupling energy densities simplify to

$$f_{E,1} = -v_1 \hat{u}_{yy} E^2, \tag{4.5a}$$

$$f_{E,2} = -KE(\tilde{c}_x + u_{xz}). \tag{4.5b}$$

In Eq. (4.5b) we have dropped higher order terms in $\tilde{c}_a$ which are inconsequential for the leading behavior since we are interested in the Sm$A^*$ and not in the Sm$C^*$ phase. For the same reason, we need, when we combine $f_{E,1}$ and $f_{E,2}$ with the remaining parts of $f$, to keep in $f_c$ and $f_{\text{coupl}}$ only terms up to second order in $\tilde{c}_a$. To keep our discussion as simple as possible, we will focus in the following on the incompressible limit. If strains are small, as we assume, we can implement this limit by setting $u_{ii}=0$. In accordance with the given geometry, we set $u_{xy}=u_{yz}=\tilde{c}_y=0$. Collecting all parts of the elastic energy density we then obtain

$$\begin{aligned} f &= f_{\text{uni}} + f_{\text{nonlin}} + f_c + f_{\text{coupl}} + f_{E,1} + f_{E,2} \\ &= \tfrac{1}{2}(C_1 + C_4)u_{zz}^2 + 2C_4(u_{xx}^2 + u_{xx}u_{zz}) + C_5 u_{az}^2 + \tfrac{1}{2}r\tilde{c}_x^2 \\ &\quad + \tfrac{1}{2}(2\lambda_1 + \lambda_3)\tilde{c}_x^2 u_{zz} - B_1 u_{zz}u_{xz}^2 + \lambda_3 \tilde{c}_x^2 u_{xx} + \lambda_4 \tilde{c}_x u_{xz} \\ &\quad + \lambda_5 u_{zz}u_{xz}\tilde{c}_x - KE(\tilde{c}_x + u_{xz}) + v_1(u_{xx} + u_{zz})E^2, \end{aligned} \tag{4.6}$$

where we have eliminated $u_{yy}$ by using $u_{ii}=0$ and where we dropped the $B_2(u_{az}^2)^2$ term.

Next, we determine the equilibrium values of the strain components and the $c$ director in the presence of the electric field. The equilibrium values $\tilde{c}_x^0$ and $u_{zx}^0$, which are at leading order linear in $E$, are

$$\tilde{c}_x^0 = \frac{2C_5 - \lambda_4}{2C_5 r_R} KE, \tag{4.7a}$$

$$u_{zx}^0 = -\frac{\lambda_4 - r}{2C_5 r_R} KE = \frac{r - \lambda_4}{2C_5 - \lambda_4}\tilde{c}_x^0, \tag{4.7b}$$

where $r_R = r - \lambda_4^2/(2C_5)$. The diagonal components of $u_{ij}^0$ can also be calculated by minimizing the free energy of Eq. (4.6). The results are that $u_{zz}^0$ and $u_{xx}^0$ both have contributions proportional directly to $E^2$ and contributions proportional to $(\tilde{c}_x^0)^2$. In addition $u_{zz}^0$ has a contribution proportional to $-B(u_{xz}^0)^2$. All of these terms are proportional to $E^2$.

The relative height change

$$\Delta h/h_0 = (h - h_0)/h_0 = u_{zz}^0 \tag{4.8}$$

of the film is

$$\begin{aligned} \Delta h/h_0 &= -\frac{1}{C_1}[\lambda_1(\tilde{c}_x^0)^2 + \lambda_5 \tilde{c}_x^0 u_{xz}^0 - B_1(u_{xz}^0)^2] - \frac{v_1}{2C_1}E^2 \\ &\approx -\frac{1}{2}[(\tilde{c}_x^0 + u_{xz}^0)^2 - 4(u_{xz}^0)^2] - \frac{v_1}{2C_1}E^2, \end{aligned} \tag{4.9}$$

where we used $B_{\text{sm}} \gg \mu, r_t$ to obtain the last form (which sets $f_{\text{layer}}=0$). The electrostriction coefficient is defined via $\Delta h/h_0 \equiv -a_{\text{el}}E^2$. Inserting Eq. (4.7) into Eq. (4.9), we obtain

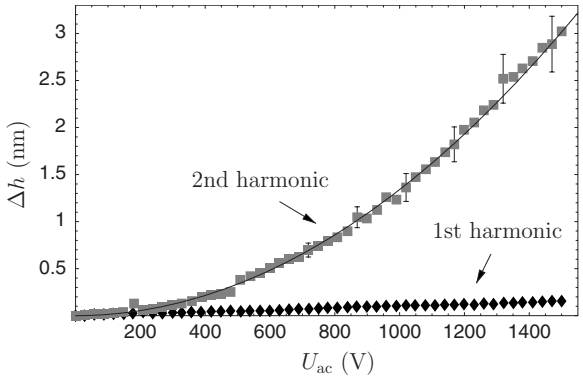


FIG. 6. Hight change of a Sm$A^*$ elastomer in response to an alternating lateral voltage $U_{\text{ac}}(t)=U_{\text{ac}}\cos(\omega t)$ as a function of the amplitude $U_{\text{ac}}$. The data points are taken from Ref. [6], where a sample of thickness $h_0=75\pm5$ nm and width $d=1$ mm was used and the frequency of the voltage was $\omega=133$ Hz. There is a small piezoelectric contribution, i.e., a contribution that is linear in $U_{\text{ac}}$ or, respectively, the amplitude of the electric field $E_{\text{ac}}(t)=U_{\text{ac}}(t)/d$. In contrast, the contribution proportional to the square of the field, i.e., the effect of electrostriction, at the second harmonic is large. The continuous curve stems from our theoretical result (4.12) with $a_{\text{el}}=7.147\times10^{-14}$ (m/V)$^2$.

$$a_{\text{el}} \approx \frac{v_1}{2C_1} + \frac{2(2p-1)}{(p+1)^2}\left(\frac{2C_5 - \lambda_4}{2C_5 r_R}K\right)^2 = \frac{v_1}{2C_1} + \frac{1}{2}\frac{2p-1}{p^2}\frac{K^2}{r_t^2}. \tag{4.10}$$

Finally, we compare our theoretical findings to the experimental results. In their experiments, Lehmann *et al.* applied alternating lateral voltage, $U_{\text{ac}}(t)=U_{\text{ac}}\cos(\omega t)$, so that $E=E_{\text{ac}}(t)=U_{\text{ac}}(t)/d$, where $d$ is the width of the sample, and they measured the first and the second harmonic of $\Delta h$. Rewriting Eq. (4.9) as

$$\Delta h = \frac{h_0 a_{\text{el}} U_{\text{ac}}^2}{4d^2}[1 + \cos(2\omega t)] + \cdots, \tag{4.11}$$

our model predicts that the amplitude $\Delta h_2$ of the second harmonic is

$$\Delta h_2 = \frac{h_0 a_{\text{el}} U_{\text{ac}}^2}{4d^2}. \tag{4.12}$$

In Fig. 6 our result (4.12) is compared to the experimental data of Lehmann *et al.* Taking the values $h_0=75\pm5$ nm and $d=1$ mm of Ref. [6] and setting $a_{\text{el}}=7.147\times10^{-14}$ (m/V)$^2$, we obtain an excellent fit between our theory and the experimental curve for the second harmonic. Likewise, we can fit our theory easily to the experimental curves of Köler *et al.* [7]. We refrain here to show the corresponding curves in order to save space. Beyond producing fitting curves, we can extract from our theory an estimate for the value of $a_{\text{el}}$. Let us start with the first term in the second line of Eq. (4.10). The coefficient $v_1$ should be of order $\epsilon_0\chi_0$, where $\epsilon_0=8.85\times10^{-12}$ Pa (m/V)$^2$ is the permeability of the vacuum and $\chi_0\approx2.5$ is the electric susceptibility. With these values, the term containing $v_1$ is of order $2\times10^{-11}/4\times10^7 \approx 0.5\times10^{-18}$ (m/V)$^2$, which is orders of magnitude smaller than

the experimental values. Now, we turn to the second term in the second line of Eq. (4.10). In accord with this term, the experiments of Lehmann *et al.* and Köler *et al.* found the largest values of $a_{\rm el}$ for temperatures near $T_c$. Based on the BZGGZ and the AD values, we estimate $r_t$ to be of the order $r_t \sim 10^4$ Pa and $r_t \sim 10^5$ Pa, respectively, for $T$ within a range of a few degrees about $T_c$. Recalling the experimental values for $K$ and that $p \approx 1$, were are led to $a_{\rm el} \approx 5 \times 10^{-15}$ $(\mathrm{m/V})^2$ for the BZGGZ values and $a_{\rm el} \approx \times 10^{-18}$ $(\mathrm{m/V})^2$ for the AD values. Perhaps not surprisingly, the latter estimate, being based on experimental data for liquid smectics, turns out poor. The estimate $a_{\rm el} \approx 5 \times 10^{-15}$ $(\mathrm{m/V})^2$ is in much better agreement with the electrostriction experiments. It is about one order of magnitude smaller than the value $a_{\rm el}=7.147 \times 10^{-14}$ $(\mathrm{m/V})^2$ obtained by fitting the data of Lehmann *et al.* and it is of the same order of magnitude as the value $a_{\rm el}=(1 \pm 0.2) \times 10^{-15}$ $(\mathrm{m/V})^2$ quoted in Ref. [7].

## V. CONCLUDING REMARKS

We have investigated the behavior of monodomain Sm*A* elastomers under strains $u_{zz}$ along the smectic layer normal. When exceeding a threshold value $u_{zz}^c$, these strains induce a transition to a Sm*C*-like state. This effect is accompanied by a tilt of the mesogenic component that sets in at the same threshold. Due to the transition, the Young's modulus $Y_{\|}$ is qualitatively different from that of conventional uniaxial elastomers: the slope of the stress-strain curve changes from high constant value for $u_{zz} < u_{zz}^c$ to a much lower constant value for $u_{zz} < u_{zz}^c$. Our results for the stress-stain behavior as well as for the layer tilt agree nicely with the available experimental data.

Moreover, we studied the electroclinic effect in Sm$A^*$ elastomers in an external, lateral electric field. Here, it is the external field that induces a transition to a Sm$C^*$-like state. Since this state is sheared in the plane perpendicular to the field, the height of a sample is lower than in the initial Sm$A^*$ phase. Our theory finds, in absolute agreement with the experimental evidence, that his height change is proportional to the square of magnitude of the external field, i.e., that the mechanism at work is the so-called electrostriction. Our numerical estimate for the electrostriction coefficient is in accord with the available experimental values.

## ACKNOWLEDGMENTS

This work was supported in part by the National Science Foundation under Grant No. DMR 0404670 (T.C.L).

## APPENDIX: NOTE ON THE WORK OF ADAMS AND WARNER

Here we will discuss the connection between the AW theory and our theory for Sm*A*'s in some more detail to understand the agreement in the results more systematically. Moreover, we will generalize the AW theory to allow for relative till between the director and the layer normal.

### 1. Comparison to the work of Adams and Warner

AW extended the neoclassic model of rubber elasticity by formulating an elastic energy density

$$f_{\rm AW} = \tfrac{1}{2}\mu\, \mathrm{Tr}[\underline{\underline{\Lambda}}\,\underline{\underline{\ell}}_0\underline{\underline{\Lambda}}^T\underline{\underline{\ell}}^{-1}] + \tfrac{1}{2}B(d/d_0 - 1)^2. \tag{A1}$$

The first term on the right hand side of Eq. (A1) is the usual trace formula of the neoclassic model. $\mu$ is the shear modulus.

$$\underline{\underline{\ell}}_0 = \underline{\underline{\delta}} + (p-1)\mathbf{n}_0\mathbf{n}_0 \tag{A2}$$

is the so-called shape tensor describing the conformations of polymeric chains before deformation and

$$\underline{\underline{\ell}}^{-1} = \underline{\underline{\delta}} - (1-p^{-1})\mathbf{nn} \tag{A3}$$

is its counterpart after a deformation has been applied. As in the main text, $p$ denotes the anisotropy ratio of the uniaxial state, which we assume to be prolate, $p>1$. The AW model assumes incompressibility, i.e., the deformation tensor is subject to the constraint $\det\underline{\underline{\Lambda}}=1$. The new element in the theory of AW, the second term on the right hand side of Eq. (A1), describes changes in the spacing of smectic layers. $B$ is a layer compression modulus. $d_0$ and $d$ are, respectively, the layer spacing before and after deformation which are related via

$$\frac{d}{d_0} = \frac{1}{|(\underline{\underline{\Lambda}}^{-1})^T\mathbf{n}_0|}. \tag{A4}$$

In the following, we chose $\mathbf{n}_0=(0,0,1)$ and we set $\mathbf{n}=(\sin\theta,0,\cos\theta)$. Assuming a deformation tensor of the form shown in Eq. (3.1), the elastic energy density becomes

$$\begin{aligned} f = \frac{1}{2}\mu\{&\Lambda_{zz}^2 + \Lambda_{xx}^2 + \Lambda_{xx}^{-2}\Lambda_{zz}^{-2} + p^{-1}\Lambda_{zx}^2(1-p^{-1})(p\Lambda_{zz}^2 - \Lambda_{xx}^2 \\ &+ \Lambda_{zx}^2)\sin^2\theta - 2(1-p^{-1})\Lambda_{xx}\Lambda_{zx}\sin\theta\cos\theta\} \\ &+ b\left(\frac{\Lambda_{zz}\Lambda_{xx}}{\sqrt{\Lambda_{xx}^2+\Lambda_{zx}^2}} - 1\right)^2, \end{aligned} \tag{A5}$$

where $\Lambda_{yy}$ has been eliminated via the incompressibility constraint, and where $b=B/\mu$. For studying the response of an Sm*A* elastomer to an imposed deformation $\Lambda_{zz}$, AW assume that $\mathbf{n}$ and $\mathbf{N}$ are locked, which amounts to setting

$$\sin\theta = -\frac{\Lambda_{zx}}{\sqrt{\Lambda_{xx}^2+\Lambda_{zx}^2}}, \quad \cos\theta = \frac{\Lambda_{xx}}{\sqrt{\Lambda_{xx}^2+\Lambda_{zx}^2}}. \tag{A6}$$

Then, the AW elastic energy density becomes

$$\begin{aligned} f_{\rm AW} = \frac{1}{2}\mu\Bigg\{&\Lambda_{xx}^2 + \frac{1}{\Lambda_{xx}^2\Lambda_{zz}^2} + \Lambda_{zx}^2 + \frac{(\Lambda_{xx}^2 + p\Lambda_{zx}^2)\Lambda_{zz}^2}{\Lambda_{xx}^2+\Lambda_{zx}^2} \\ &+ b\left(\frac{\Lambda_{xx}\Lambda_{zz}}{\sqrt{\Lambda_{xx}^2+\Lambda_{zx}^2}} - 1\right)^2\Bigg\}. \end{aligned} \tag{A7}$$

In order to make contact to our Lagrangian theories, we re-express the components of the deformation tensor in terms of the components of the strain tensor. From the definition of the strain tensor and Eq. (3.1) it is straightforward to see that the respective components are related by

$$\Lambda_{yy} = \sqrt{1 + 2u_{yy}}, \tag{A8a}$$

$$\Lambda_{zz} = \sqrt{1 + 2u_{zz}}, \tag{A8b}$$

$$\Lambda_{zx} = u_{xz}/\Lambda_{zz}, \tag{A8c}$$

$$\Lambda_{xx} = \sqrt{1 + 2u_{xx} - \Lambda_{zx}^2}. \tag{A8d}$$

Inserting Eq. (A8) into the elastic energy density (A7) to eliminate the $\Lambda_{ij}$ and then expanding in powers of the $u_{ij}$ we obtain

$$f_{\mathrm{AW}} = \mu\left\{\frac{3}{2} + \frac{4+b}{2}u_{zz}^2 + 2u_{zz}u_{xx} + 2u_{xx}^2 + \frac{p}{2}u_{zx}^2 - \frac{4+b}{2}u_{zz}u_{zx}^2 - (1+p)u_{xx}u_{zx}^2 + \frac{4+b}{2}u_{zx}^4\right\}, \tag{A9}$$

where we have dropped higher order terms which are inconsequential for the argument here.

Next, we revisit elastic energy density $f$ in Eq. (2.3). To obtain a model in terms of strain only, we integrate $\tilde{c}_a$ out of $f$. This procedure leads to

$$f = f_{\mathrm{uni}} + D_1 u_{zz}u_{az}^2 + D_2 u_{ii}u_{az}^2 + D_3 \hat{u}_{ab}u_{az}u_{bz} + G(u_{az}^2)^2, \tag{A10}$$

with $C_5$ renormalized to $C_5^R$ [see Eq. (2.9)] in $f_{\mathrm{uni}}$, with $D_m = \lambda_m\lambda_4^2/r$ for $m=1,2,3$, and $G=(g/4+r/2)\lambda_4^4/r^4$. Then, we carry out the following steps: (i) we implement the incompressible limit via the constraint $u_{ii}=0$ so that the terms featuring $C_2$, $C_3$, and $D_2$ are absent, (ii) we eliminate $u_{yy}$ with help of $u_{ii}=0$, and (iii) we assume a deformation tensor of the form (3.1) so that $u_{xy}=u_{yz}=0$. Then, $f$ reduces to

$$f = \tfrac{1}{2}(C_1 + C_4)u_{zz}^2 + 2C_4u_{zz}u_{xx} + 2C_4u_{xx}^2 + C_5^R u_{zx}^2 + \left(D_1 + \tfrac{1}{2}D_3\right)u_{zz}u_{zx}^2 + D_3u_{xx}u_{zx}^2 + Gu_{zx}^4, \tag{A11}$$

which has, with the exception lacking the inconsequential constant term, exactly the same form as $f_{\mathrm{AW}}$. Comparison of the individual terms in Eqs. (A9) and (A11) reveals that the elastic constants in the two models are related by $C_1=\mu(3+b)$, $C_4=\mu$, $C_5^R=p\mu$, $D_1=\mu(p-3-b)/2$, $D_3=-\mu(1+p)$, and $G=\mu(4+b)/8$. Note that AW work with the values $b=5$ and $p=2$ which corresponds to negative values of $D_1$ and $D_3$.

The effective elastic energy density in terms of $u_{zz}$ only produced by Eq. (A11) is essentially the same as the incompressible limit of Eq. (3.17). Thus, in the end, the AW model and our models lead, at least to leading order, to the same stress-strain curve, see Fig. 4.

### 2. Extending the model of Adams and Warner

Now we generalize the AW model by avoiding the assumption that the layer normal and the director are locked. The full elastic energy density (A5) rather than the AW elastic energy density (A7) will be the vantage point for the following considerations. In the remainder, we abbreviate $\Lambda \equiv \Lambda_{zz}$ for notational simplicity.

We can reduce Eq. (A5) to a function of $\Lambda$, $\Lambda_{xx}$, and $\Lambda_{zx}$ only by minimizing over $\theta$. The result is

$$\sin\theta = \sqrt{\frac{1}{2}\left[1 - \sqrt{1 + \frac{\mathcal{B}^2}{\mathcal{A}^2}}\right]}, \tag{A12a}$$

$$\cos\theta = \sqrt{\frac{1}{2}\left[1 + \sqrt{1 + \frac{\mathcal{B}^2}{\mathcal{A}^2}}\right]}, \tag{A12b}$$

where

$$\mathcal{A} = p\Lambda^2 + \Lambda_{zx}^2 - \Lambda_{xx}^2, \tag{A13a}$$

$$\mathcal{B} = 2\Lambda_{xx}\Lambda_{zx}. \tag{A13b}$$

The free energy minimized over $\theta$ is then

$$f_m = \frac{1}{2}\mu\left\{(1+p)\Lambda^2 + (1+p^{-1})\Lambda_{xx}^2 + 2\Lambda^{-1}\Lambda_{xx}^{-2} + (1+p^{-1})\Lambda_{zx}^2 - (1-p^{-1})\sqrt{(r\Lambda^2 - \Lambda_{xx}^2 + \Lambda_{zx}^2)^2 + 4\Lambda_{xx}^2\Lambda_{zx}^2}\,] + b\left(\frac{\Lambda\Lambda_{xx}}{\sqrt{\Lambda_{xx}^2 + \Lambda_{zx}^2}} - 1\right)^2\right\}. \tag{A14}$$

To determine instabilities toward the development of $\Lambda_{zx}$, we expand $f_m$ to second order in $\Lambda_{zx}$:

$$f_m \approx \frac{1}{2}\mu[p\Lambda^2 + \Lambda_{xx}^2 + \Lambda^{-2}\Lambda_{xx}^{-2}] + b(\Lambda - 1)^2 + \frac{1}{2}\mu\left(\frac{\Lambda^2 - \Lambda_{xx}^2}{p\Lambda^2 - \Lambda_{xx}^2} - 2b\frac{\Lambda(\Lambda-1)}{\Lambda_{xx}^2}\right)\Lambda_{zx}^2. \tag{A15}$$

Now we minimize this function over $\Lambda_{xx}$ at $\Lambda_{zx}=0$. The result is $\Lambda_{xx}=\Lambda^{-1/2}$. Thus, when $\Lambda=1$, $\Lambda_{xx}=1$, $\Lambda_{xx}^2=\Lambda^2$, and the coefficient of $\Lambda_{zx}$ is zero, i.e., there is no restoring force for infinitesimal shear strains in this model of smectics. The origin of this behavior is the invariance of both terms in the free energy with respect to rotations. Semisoft terms need to be added to endow the smectic layers with a preferred direction relative to the crosslinked matrix. Next, we consider what happens when $\Lambda > 1$. The coefficient of $\Lambda_{zx}^2$ becomes

$$A_{zx} = -\frac{1}{2}\mu(\Lambda - 1)\left(b\Lambda^2 - \frac{\Lambda^2 + \Lambda + 1}{p\Lambda^3 - 1}\right). \tag{A16}$$

This terms is negative for all $\Lambda > 1$ because $b \gg 1$. Thus, in the absence of a semisoft term, there is no threshold for the production of shear strain in response to an imposed strain along the $z$ direction.

As we have just seen, there is an instability to transfer shear for all $\Lambda > 1$ in the original AW theory if the nematic director is allowed to relax. Thus, the model elastic energy density (A5) is insufficient to produce stress-strain curves as measured by NF. The problem is that this model is invariant with respect to simultaneous rotations of the smectic layers, the nematic director, and $\Lambda$ in the target space. To break this invariance, we introduce the semisoft energy

$$f_{\mathrm{semi}} = \frac{1}{2}\mu\alpha\,\mathrm{Tr}[(\underline{\underline{\delta}} - \mathbf{n}_0\mathbf{n}_0)\underline{\underline{\Lambda}}^T\mathbf{n}\mathbf{n}\underline{\underline{\Lambda}}] \tag{A17}$$

$$= \frac{1}{2}\mu\alpha(\Lambda_{xx}\sin\theta + \Lambda_{zx}\cos\theta)^2. \tag{A18}$$

The complete energy is then

$$f_T = f + f_{\text{semi}}. \tag{A19}$$

Expanding to second order in $\theta$, we obtain

$$f = \frac{1}{2}\mu\Big\{\Lambda^2 + \Lambda_{xx}^2 + \Lambda_{xx}^{-2}\Lambda^{-2} + (p^{-1}+\alpha)\Lambda_{zx}^2 - 2(1-p^{-1}-\alpha)\Lambda_{xx}\Lambda_{zx}\theta + [(1-p^{-1})(p\Lambda^2 - \Lambda_{xx}^2 + \Lambda_{zx}^2) + \alpha(\Lambda_{xx}^2 - \Lambda_{zx}^2)]\theta^2 + b\left(\frac{\Lambda\Lambda_{xx}}{\sqrt{\Lambda_{xx}^2+\Lambda_{zx}^2}} - 1\right)^2\Big\}. \tag{A20}$$

Minimizing over $\theta$, we obtain

$$\theta = \frac{(1-p^{-1}-\alpha)\Lambda_{xx}\Lambda_{zx}}{(1-p^{-1})(p\Lambda^2 - \Lambda_{xx}^2 + \Lambda_{zx}^2) + \alpha(\Lambda_{xx}^2 - \Lambda_{zx}^2)} \tag{A21}$$

and a relaxed free energy to harmonic order in $\Lambda_{zx}$ of

$$f_m \approx \frac{1}{2}\mu[p\Lambda^2 + \Lambda_{xx}^2 + \Lambda^{-2}\Lambda_{xx}^{-2}] + b(\Lambda-1)^2 + \frac{1}{2}\mu\left[\frac{(p-1)(\Lambda^2 - \Lambda_{xx}^2) + p\alpha[(p-1)\Lambda^2 + \Lambda_{xx}^2]}{(p-1)(p\Lambda^2 - \Lambda_{xx}^2) + \alpha\Lambda_{xx}^2} - 2b\frac{\Lambda(\Lambda-1)}{\Lambda_{xx}^2}\right]\Lambda_{zx}^2. \tag{A22}$$

The term of order 0 in $\Lambda_{zx}$ has the same form as it did in the absence of the semisoft term. Thus, as before, $\Lambda_{xx} = \Lambda^{-1/2}$, and the coefficient of $\Lambda_{zx}^2$ is

$$A = \frac{\mu}{2}\left[\frac{(p-1)(\Lambda^3-1) + \alpha p[(p-1)\Lambda^3 + 1]}{(p-1)(p\Lambda^3 - 1) + \alpha p} - 2b\Lambda^2(\Lambda-1)\right]. \tag{A23}$$

If $\Lambda = 1 + u_{zz}$, then to lowest order in $u_{zz}$,

$$A = \frac{\mu}{2}\left[\frac{\alpha p^2}{(p-1)^2 + \alpha p} - 2bu + \frac{3(p-1)(p(\alpha-1)+1)^2}{((p-1)^2 + p\alpha)^2}u\right], \tag{A24}$$

and thus there is a nonzero the critical value of the strain $u_{zz}$,

$$u_{zz}^c = \frac{p^2\alpha[(1-p)^2 + p\alpha]}{2b[(1-p)^2 + p\alpha] - 3(p-1)[p(\alpha-1)+1]^2}, \tag{A25}$$

in accord with the experiments of NF and our Lagrangian theory. Note that this critical strain is linearly proportional to $\alpha$ at small $\alpha$ and vanishes as $\alpha \to 0$ in agreement with our previous observation that the elastomer is unstable to shear at infinitesimal strain along $z$ if it is soft rather than semisoft. Having $u_{zz}^c$, we can proceed to calculate the entire stress-strain curve. The result is in full qualitative agreement with the experimental curves and the predictions of our Lagrangian theory. To save space, we leave the remaining steps as an exercise to the reader.


[1] For a review on liquid crystal elastomers see W. Warner and E. M. Terentjev, *Liquid Crystal Elastomers* (Clarendon Press, Oxford, 2003).

[2] For a review on liquid crystals see P. G. de Gennes and J. Prost, *The Physics of Liquid Crystals* (Clarendon Press, Oxford, 1993); S. Chandrasekhar, *Liquid Crystals* (Cambridge University Press, Cambridge, 1992).

[3] E. Nishikawa and H. Finkelmann, Macromol. Chem. Phys. **200**, 312 (1999).

[4] W. Helfrich, Appl. Phys. Lett. **17**, 531 (1970); J. Chem. Phys. **55**, 839 (1971); J. P. Hurault, J. Chem. Phys. **59**, 2068 (1973).

[5] N. Clark and R. Meyer, Appl. Phys. Lett. **22**, 493 (1973).

[6] W. Lehmann *et al.*, Nature (London) **410**, 447 (2001).

[7] R. Köhler, R. Stannarius, C. Toklsdorf, and R. Zentel, Appl. Phys. A **80**, 381 (2003).

[8] O. Stenull and T. C. Lubensky, Phys. Rev. Lett. **94**, 018304 (2005).

[9] O. Stenull and T. C. Lubensky, Phys. Rev. E **74**, 051709 (2006).

[10] L. D. Landau and E. M. Lifshitz, *Theory of Elasticity*, 3rd ed. (Pergamon Press, New York, 1986).

[11] P. M. Chaikin and T. C. Lubensky, *Principles of Condensed Matter Physics* (Cambridge Press, Cambridge, 1995).

[12] J. M. Adams and M. Warner, Phys. Rev. E **71**, 021708 (2005).

[13] E. M. Terentjev and M. Warner, J. Phys. II **4**, 111 (1994).

[14] E. M. Terentjev and M. Warner, J. Phys. II **4**, 849 (1994).

[15] See, e. g., R. A. Horn and C. R. Johnson, *Topics in Matrix Analysis* (Cambridge University Press, New York, 1991).

[16] The vector $\tilde{\mathbf{e}}$ is identical to the anisotropy vector $\mathbf{n}_0$ at the time of crosslinking used in the work of Warner, Terentjev, and collaborators (as in Ref. [1]). $\mathbf{n}_0$ couples to the left-hand index of $\Lambda_{ij}$ and is a reference-space vector that sets the anisotropy direction of the reference material.

[17] J.-H. Chen and T. C. Lubensky, Phys. Rev. A **14**, 1202 (1976).

[18] M. Brehmer, R. Zentel, F. Gieselmann, R. Germer, and P. Zungenmaier, Liq. Cryst. **21**, 589 (1996).

[19] P. Archer and I. Dierking, Phys. Rev. E **72**, 041713 (2005).